



NRC Publications Archive Archives des publications du CNRC

Quantitative measurements at three and ten centimeters of radar echo intensities from precipitation Hood, A.D.

For the publisher's version, please access the DOI link below./ Pour consulter la version de l'éditeur, utilisez le lien DOI ci-dessous.

<https://doi.org/10.4224/21272332>

NRC Publications Record / Notice d'Archives des publications de CNRC:

<https://nrc-publications.canada.ca/eng/view/object/?id=ea45a539-5bee-4861-b5be-720ddaba867d>
<https://publications-cnrc.canada.ca/fra/voir/objet/?id=ea45a539-5bee-4861-b5be-720ddaba867d>

Access and use of this website and the material on it are subject to the Terms and Conditions set forth at

<https://nrc-publications.canada.ca/eng/copyright>

READ THESE TERMS AND CONDITIONS CAREFULLY BEFORE USING THIS WEBSITE.

L'accès à ce site Web et l'utilisation de son contenu sont assujettis aux conditions présentées dans le site

<https://publications-cnrc.canada.ca/fra/droits>

LISEZ CES CONDITIONS ATTENTIVEMENT AVANT D'UTILISER CE SITE WEB.

Questions? Contact the NRC Publications Archive team at

PublicationsArchive-ArchivesPublications@nrc-cnrc.gc.ca. If you wish to email the authors directly, please see the first page of the publication for their contact information.

Vous avez des questions? Nous pouvons vous aider. Pour communiquer directement avec un auteur, consultez la première page de la revue dans laquelle son article a été publié afin de trouver ses coordonnées. Si vous n'arrivez pas à les repérer, communiquez avec nous à PublicationsArchive-ArchivesPublications@nrc-cnrc.gc.ca.



National Research
Council Canada

Conseil national de
recherches Canada

Canada

Ser
QC1
N21
ERA 180
c. 2

ERA - 180

UNCLASSIFIED

ANALYZED

NATIONAL RESEARCH COUNCIL OF CANADA
RADIO AND ELECTRICAL ENGINEERING DIVISION

QUANTITATIVE MEASUREMENTS AT
THREE AND TEN CENTIMETERS OF RADAR ECHO INTENSITIES
FROM PRECIPITATION

BY

A. D. HOOD

OTTAWA

JUNE 1950

N.R.C. NO. 2155

QUANTITATIVE MEASUREMENTS AT
THREE AND TEN CENTIMETERS OF RADAR ECHO INTENSITIES
FROM PRECIPITATION

by

A.D. Hood

Intro:	3
Text:	15
Figs:	15
Photos:	7

ABSTRACT

Permanent rainstorm records were produced by photographing radar type-A displays in conjunction with the recording of meteorological data. The analysis has proved that the rate of fall in rainstorms can be measured by radar with reasonable accuracy.

Simultaneous quantitative measurements at three and ten centimeters agree with both theory and previous experimental results showing that radar echoes are dependent on drop size distribution, and are proportional to the sum of the sixth power of the drop diameters contained in a unit volume.

Quantitative measurements have given an absolute comparison of X-band and S-band performance and have illustrated the limitations of X-band as a useful frequency in meteorological work. The data may be applied to any radar to estimate the detection ranges of typical targets in rainstorms.

CONTENTS

	<u>Page</u>
I INTRODUCTION	1
II THEORY	1
III LOCATION AND EQUIPMENT	7
IV THE EXPERIMENT	9
V CONCLUSIONS	14
VI ACKNOWLEDGMENT	14
REFERENCES	15

QUANTITATIVE MEASUREMENTS AT THREE AND TEN CENTIMETERS OF RADAR ECHO INTENSITIES FROM PRECIPITATION

I

INTRODUCTION

A great deal of work has been carried out on radar storm detection and echo intensities from precipitation. Very little of this work, however, has consisted of absolute quantitative measurements. It is relatively simple to make a qualitative analysis of radar echoes from precipitation, whereas measurement of the absolute power received requires accurate and continuous radar calibration in correlation with accurate meteorological data.

This report deals with one phase of radar meteorological work, that of measuring quantitatively the echo intensity from rain in a horizontal radar beam. Measurements of rain clutter signals taken from simultaneous photographic records of X-band and S-band radars provide a comparison of the two bands for use in (a) meteorological work, (b) radar search and navigation in ideal or adverse weather conditions.

II

THEORY

The back-scattered energy from precipitation in a radar beam is a function of drop size and the rate of fall, with drop size assuming increasing importance as the wavelength decreases from ten centimeters. While drop size bears a certain relationship to the rate of fall, the existing data listing typical values of drop size for given precipitation rates is not sufficiently accurate for determining the precipitation quantity important to radar. This quantity $\sum D^6$ (sum of the diameters to the sixth power of the drops per unit volume) must be determined by experimental means. Several methods are available but the dyed-filter-paper technique has been used throughout this experiment.

The scattering theory has been taken mainly from the reports of J.W. Ryde. Ryde's simplified equations, for use when drop diameters are small compared with the wavelength, are permissible for all ten-centimeter measurements. The same equations are not so appropriate in the case of large drops at three centimeters and the general formula must be used.

The theory pertaining to the quantitative measurement of radar echo intensities is covered by the development of the following expressions:

- (a) I_r The echo intensity back-scattered from one drop of water at distance r .
- (b) $f_0(d, m)$ The scattering function — depending on $d = \frac{\pi D}{\lambda}$, in which D is the drop diameter, and on m , which is a function of the refractive index and the absorption index of water.
- (c) Computation of $\sum D^6$
- (d) Radar equation involving $\sum D^6$

(a) Expression for Echo Intensities

Assuming the radar transmitter as a point source emitting a conical beam having a semi-angle, θ , if

I_1 is the intensity of radiation at unit distance, and

I_r is the intensity of radiation back-scattered from one drop of water at distance δr , then,

$$I_r = \frac{I_1}{r^2} \cdot \frac{B_1}{r^2}, \quad (1)$$

where B_1 is the scattering function depending on the wavelength of the emitted energy and on the drop size and dielectrics. If there are N drops per unit volume, the echo intensity I_r from the drops lying in a spherical shell of thickness r (centered at the source) and intersected by the beam is

$$I_r = \frac{I_1 N B_1}{r^4} \cdot 2\pi r^2 (1 - \cos \theta) \delta r.$$

Integrating over the pulse length h , when the center of the pulse is at distance r ,

$$r_1 = r - \frac{h}{2} \quad r_2 = r + \frac{h}{2}$$

$$I_r = I_1 N B_1 \cdot 2\pi (1 - \cos \theta) \int_{r_1}^{r_2} \frac{\delta r}{r^2}$$

$$= I_1 N B_1 \cdot \frac{2\pi (1 - \cos \theta)}{\frac{r^2}{h} - \frac{h}{4}}. \quad (2)$$

Ryde shows that

$$B_1 = \left(\frac{\lambda}{2\pi} \right)^2 f_0(a, m)$$

where λ is the wavelength, and $f_0(a, m)$ is a function depending on $a = \frac{\pi D}{\lambda}$ where D is the drop diameter, and on m , which is a function of the refractive and absorption indices of water.

Assuming $r \gg h$, then

$$\frac{r^2}{h} - \frac{h}{4} \approx \frac{r^2}{h}$$

Substituting in Equation (2),

$$I_r = I_1 h \lambda^2 \cdot \frac{1 - \cos \theta}{2\pi r^2} \cdot N f_0(a, m) \quad (3)$$

(b) Expression for the Scattering Function

From electromagnetic theory, Ryde has developed the general expression for the scattering function, for energy back-scattered towards the source:

$$f_0(a, m) = \frac{a}{4} \left(\left[q_1 + (q_2 - u_1 - w_1)a^2 - q_3a^3 \right]^2 + \left[r_1 + (r_2 - v_1 - w_2)a^2 - r_3a^3 \right]^2 \right) \quad (4)$$

where q_1, q_2 , etc., are functions of g and h (h bears no relationship to pulse length in Equation (3)) and g and h are functions of drop diameter and rate of fall.

For Equation (4) Ryde gives the values of q_1, q_2 , etc., in terms of g and h and lists numerical values for various frequencies. The values for X-band and S-band are as follows:

Terms	S-band	X-band
q_1	1.928	1.925
q_2	1.10	1.12
q_3	.0124	.0525
r_1	.0096	.0409
r_2	.0058	.0314
r_3	1.236	1.238
u_1	.1618	.1621
v_1	.000675	.00286
w_1	5.11	3.82
w_2	.693	2.106

Substituting S-band values in Equation (4), and making q as large as possible for rain ($q = 0.157$ for a drop diameter of 5 mm. Larger drop diameters may form but normally break up when falling) with negligible error, the second and third terms in each bracket may be neglected, and,

$$f_o(a,m) = \frac{q^6}{4} (q_1^2 + r_1^2) \quad (5)$$

$$= q^6 \frac{(g-1)^2 + h^2}{(g+2)^2 + h^2} \quad (6)$$

$$= q^6 f_o(g,h) \quad (7)$$

$$= \left(\frac{\pi}{\lambda}\right)^6 \cdot D^6 \cdot f_o(g,h) \quad (8)$$

Substituting for X-band, it is found that for $\frac{D}{\lambda} > 0.03$ (1 mm. drop dia.) the approximate Equation (5) is not sufficiently accurate and the general Equation (4) must be used. Assuming very small drops ($D < 1$ mm. dia.), Equation (5) gives a value $f_o(g,h) = 0.93$. Using the general Equation (4) with a drop size of 2.3 mm., the value of $f_o(g,h)$ is reduced to 0.777. These values calculated from Equation (4) have been used in all X-band measurements.

(c) Computation of $\sum D^6$

$\sum D^6$ was computed from filter paper samples and rain gauge readings according to the following development:

Let $N_D \delta D$ be the number of drops of diameter between $D - \frac{\delta D}{2}$ and $D + \frac{\delta D}{2}$ in unit volume

$N_{GD} \delta D$ the number falling through horizontal area in unit time
 $N_P \delta D$ the number falling on the filter paper of area A in unit time
 V_D vertical velocity of a drop of the above diameter (see Fig.1)
 R total volume of water arriving at unit horizontal area in unit time.

The quantity $\sum D^6$ (sum of the sixth power of the diameters of the drops in unit volume) appears in the radar equation for echoes from rain, and using the above symbols

$$\sum D^6 = \sum N_D D^6 \delta D.$$

But $N_{GD} \delta D = N_D V_D \delta D$,

$$\therefore \sum D^6 = \sum \frac{N_{GD} D^6}{V_D} \delta D.$$

Also $N_P \delta D = A_t N_{GD} \delta D$,

$$\therefore \sum D^6 = \frac{1}{A_t} \sum \frac{N_P D^6 \delta D}{V_D}.$$

The exposure time (t) is difficult to measure and greater accuracy can be obtained by determining A_t from R (rate of fall) and the relation

$$\begin{aligned} R &= \frac{\pi}{6} \sum N_{GD} D^3 \delta D \\ &= \frac{\pi}{6} \sum \frac{N_P D^3 \delta D}{A_t} \end{aligned}$$

$$\text{or } \frac{1}{A_t} = \frac{R}{\frac{\pi}{6} \sum N_P D^3 \delta D},$$

$$\text{and } \sum D^6 = \frac{R \sum \frac{N_P D^6}{V_D} \delta D}{\frac{\pi}{6} \sum N_P D^3 \delta D} \quad (9)$$

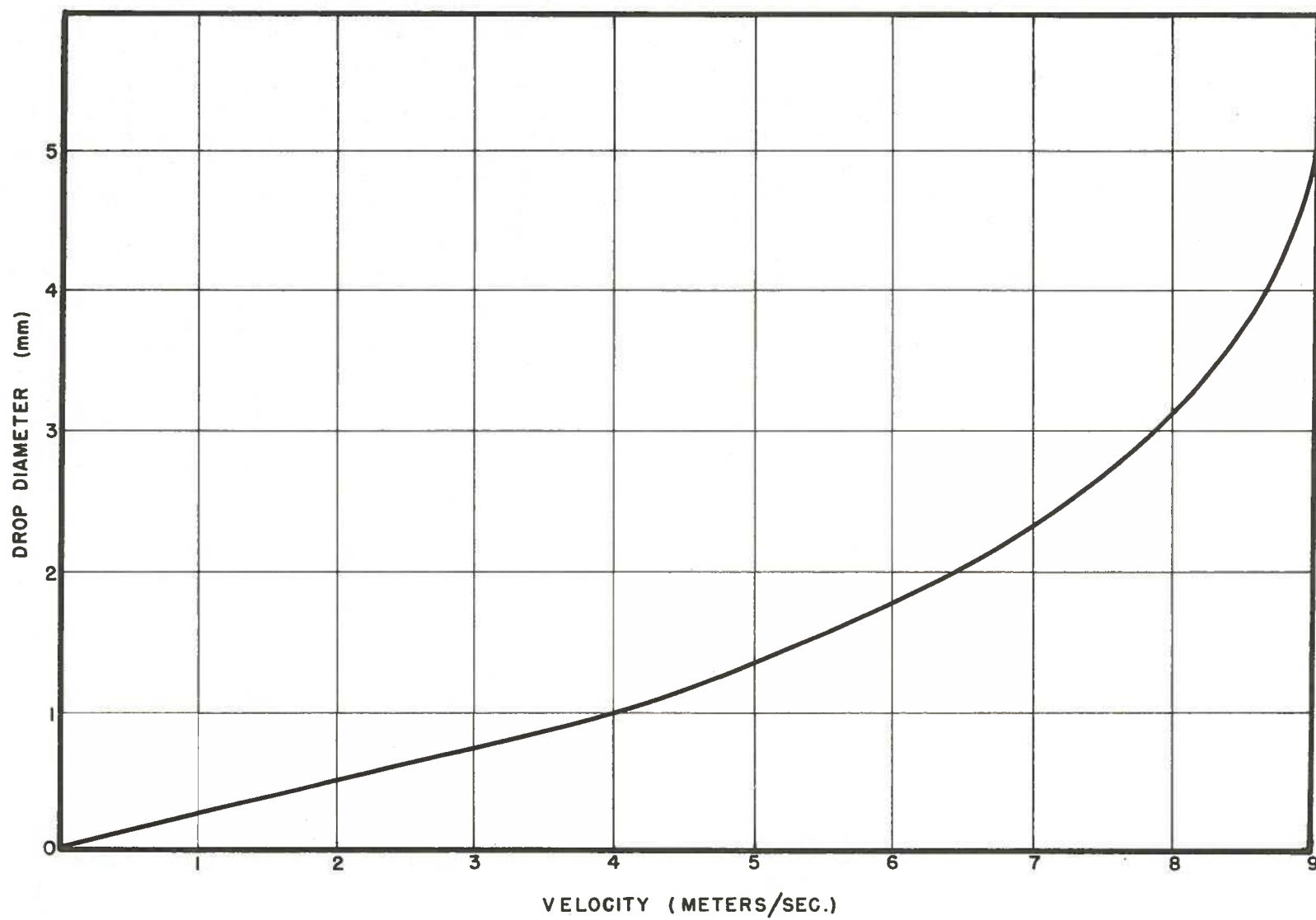


FIG. 1

TERMINAL VELOCITY OF RAINDROPS
FROM DATA BY E.D. SMITH (REF.(4))

Converting Equation (8) to practical units,

$$\begin{aligned} R &= \text{mm. per hour} \\ D &= \text{mm.} \\ V &= \text{meters per second} \\ \Sigma D^6 &= \text{mm}^6 \text{ per cubic meter} \end{aligned}$$

and including $\frac{\pi}{6}$ in the numerical factor,

$$\Sigma D^6 = 530 \frac{R \Sigma \frac{N_P D^6}{V_D} \delta D}{\Sigma N_P D^3 \delta D} \quad (10)$$

(d) Radar Expression Involving ΣD^6

From Equation (3), I is the intensity received at the radar from N drops per unit area at distance r ,

$$I_r = I_1 h \lambda^2 \cdot \frac{1 - \cos \theta}{2\pi r^2} \cdot N f_o(a, m)$$

where I_1 is intensity per unit area at unit distance from the source.

Substituting Equation (6) for the scattering function,

$$I_r = I_1 \frac{\pi^5 h (1 - \cos \theta)}{2r^2 \lambda^4} \cdot f_o(g, h) \Sigma D^6. \quad (11)$$

If P_o is power output of the radar, then

$$I_1 = \frac{P_o}{4\pi(1 - \cos \theta)}, \quad (12)$$

where I_r is intensity received per unit area.

If P_r is power received at the antenna, then

$$I_r = \frac{P_r}{A_e}, \quad (13)$$

where A_e is the effective area of the antenna.

Substituting Equations (12) and (13) in Equation (11),

$$\frac{P_r}{P_o} = \frac{\pi^4}{8} \cdot \frac{A_e h}{r^2 \lambda^4} \cdot f_o(g, h) \Sigma D^6. \quad (14)$$

A more convenient form is obtained by the following transfer of units:

A_e from centimeters² to meters²
 h from centimeters to kilometers
 r from centimeters to yards
 N from drops per cm.³ to drops per m.³
 D from centimeters to meters
 ΣD^6 is now mm.⁶ per m.³

$$\text{Then, } P_r = 14.58 \times 10^{-7} \cdot \frac{A_e h P_o}{\lambda^4} \cdot \frac{f_o(g, h) \Sigma D^6}{r^2} . \quad (15)$$

III

LOCATION AND EQUIPMENT

The radar path used in the experiment is shown in plan and elevation in Fig. 2. The radar equipment was located at the Scarboro site and the observation posts for rain measurements are shown on the radar path due east from Scarboro. The terrain of the lake shore eliminates any possibility of reflected energy reaching the field strength recorder located at Rouge Hill (Photo 1).

X-BAND RADAR (Photo 2)

Radar	Type-268, Marine
Frequency	9760 mc.
Power output	7.5 kw.
Recurrence freq.	500
Pulse length	3/4 μ sec.
Antenna	30-in. parabolic dish (Photo 4)
Antenna feed	Wave guide dipole
Polarization	Horizontal
S.W.R.	1.4
Receiver bandwidth	5 mc.
Receiver gain	72 dbm.

S-BAND RADAR (Photo 3)

Radar type	RX/C Marine
Frequency	3000 mc.
Power output	30 kw.
Recurrence freq.	500
Pulse length	1 μ sec.
Antenna	72-in. parabolic dish (Photo 4)
Antenna feed	Wave guide dipole
S.W.R.	1.5
Receiver bandwidth	8 mc.
Receiver gain	74 dbm.

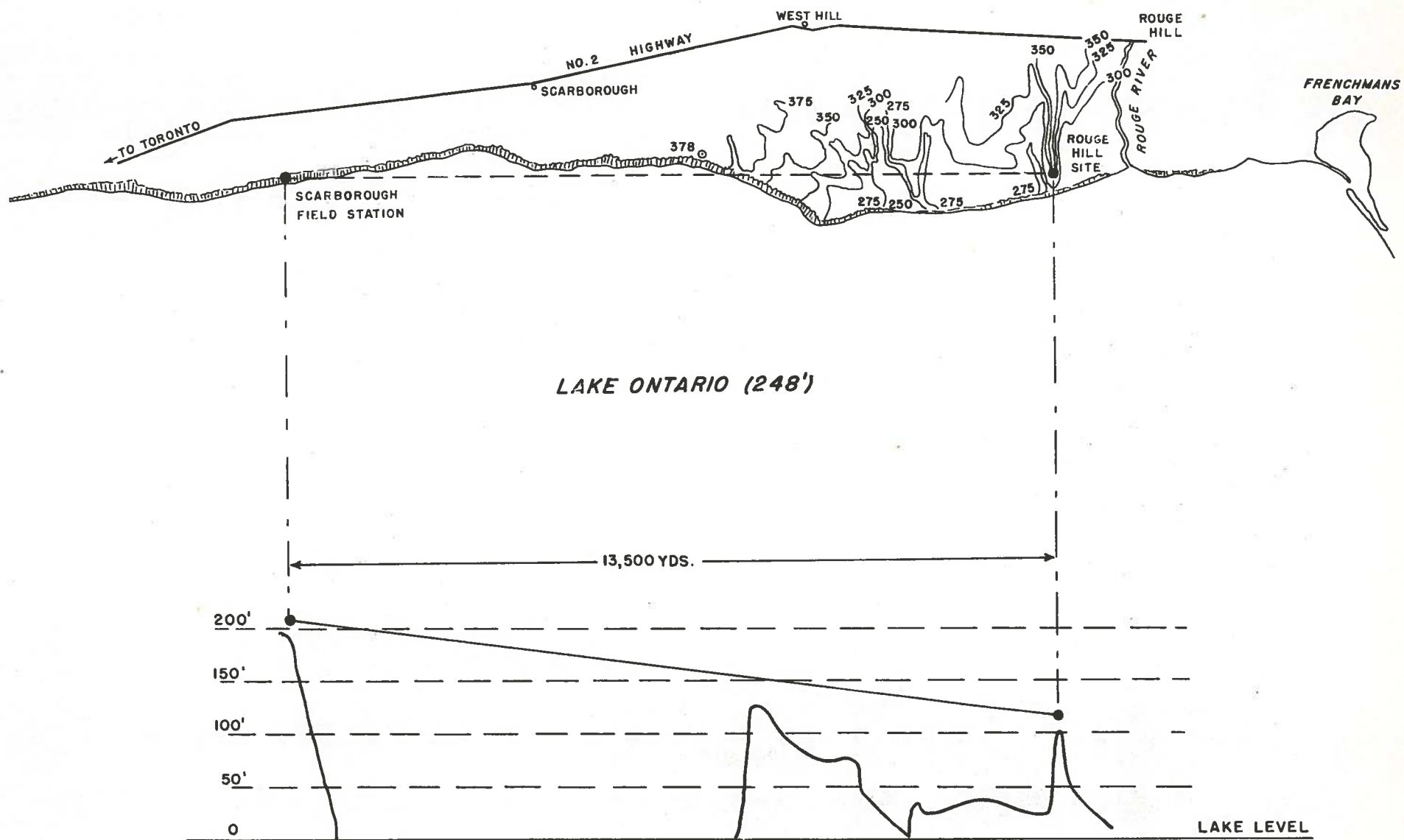


FIG. 2

X/S TRIALS

PROPAGATION PATH AND VERTICAL PROFILE

The X-band radar was calibrated with an M.I.T. pulse signal generator, type-TGX-4BL. Pulsed output from the generator, at 9760 megacycles, was coupled to the radar ahead of the mixer through a 14.5-decibel directional coupler. A $3/4$ -microsecond pulse, calibrated in decibels below a milliwatt (dbm), was thus attained on the A-scan trace and used for measuring receiver gain and echo intensity. This pulse is shown on all photographs behind a lined grid. The type-TGX-4BL frequency meter and thermistor bridge provided frequency and power output monitoring while the experiment was in progress.

The S-band radar was calibrated using a similar 10-centimeter pulse signal generator type-TGS-5BL, through a 27-decibel directional coupler. Frequency measurements were made with an absorption-type wavemeter and the power output was monitored with an external thermistor bridge.

The standing wave ratio was measured on both radars using bi-directional couplers. These measurements were made at the magnetron end of the r-f system.

An eight-foot corner reflector was located at the Rouge Hill site (Photo 7) to give a permanent echo for checking radar performance, measuring relative attenuation, and fixing antenna bearings.

Two-meter portable transceivers were used for communication, and to connect all observation posts with the Scarboro station for synchronizing time and checking the progress of approaching storms.

Photographic Equipment

Bell and Howell 35-millimeter cameras, adapted for single-frame exposure, were used to photograph X-band and S-band radar type-A displays simultaneously. The cameras were triggered automatically by rotary solenoids, controlled by Industrial timers. The time interval between frames was 28 seconds and the exposure time 2 seconds, giving 120 frames or 8 feet of film per hour. The exposure time was made as long as possible to integrate echo fluctuations. Small sweep-second watches were placed under the A-scan trace, for the purpose of synchronizing the photographed record with the observed meteorological data.

Meteorological Equipment

The rain gauges (Photo 5) were constructed from plans obtained from the Meteorological Division of the Department of Transport. A five-inch-diameter collector and a one-half-inch-diameter glass tube gave an area ratio of 100 to 1. The glass tube was graduated so that one division per minute was equivalent to one millimeter per hour of rain. A Nifer screen was placed around the collector tube to compensate for oblique rainfall. The screen was made from 9-inch tubing 15 inches long, and flared at the top to 24 inches in a parabolic curve. The curved section at

the top was covered with fine wire mesh to prevent splash into the collector. The graduated scales were illuminated with fluorescent tubes and recordings were made from inside the observation huts with mounted telescopes.

A second system was used for measuring the rate of fall (Photo 6). This was patterned after the densitometer technique using a spotlight and a photoelectric tube over a 200-foot path. A 300-watt light was modulated at the source, at 90 cycles per second, with a motor driven disk with circular holes. A lens system was focussed on the cathode of a type-929 phototube and the amplified output was used to operate a 1-milliampere Esterline Angus recorder. Calibration of the recorder was carried out by means of rain gauges along the light path. The only deficiency in this type of rate recorder is the inability of the system to distinguish between precipitation and fog.

The filter-paper technique used in obtaining values of ΣD^6 was as follows. Whatman no.1 filter paper (dia. 24 cm.) was covered with a trace of powdered gentian violet dye. The papers were stapled in cardboard folders and immediately after exposure were stamped with an automatic timer. The exposure time was varied to allow approximately 200 drops to collect on each paper. The stains caused by the drops were a function of the actual drop diameter (Fig.5). A more detailed description of this method may be obtained in Ref.1.

IV

THE EXPERIMENT

The radar equipment was installed at the Scarboro station, and the observation points located, in the summer of 1947. Experiments were conducted during the fall, but lack of suitable rainfall prevented any records of value from being taken. Considerable experience in methods of operation was obtained and the necessity for intermediate observation points became apparent. These were installed in the spring of 1948 and experiments were carried out until the following December. During this period thirteen rainstorms were recorded and photographed, and seven of these were such that conclusions could be drawn from them.

During periods of rainy weather contact was maintained with the Toronto meteorological office for advance information. Approximately one-half hour was required for the observers to reach their posts and establish radio communication. During this period the radar equipment had become stabilized and calibration was completed. Observers' watches were synchronized with the camera time.

The radar output was reduced for experiments to approximately one-half the maximum. This was found to give more stable operation over long periods and power monitor records show only one-half decibel

variation in periods of two to four hours. This figure is within the limits of accuracy of the power monitoring equipment. Power was monitored every fifteen minutes during operations.

The calibration signal from the pulse generator was at 52 dbm. on the X-band radar and 53.5 dbm. on the S-band radar. This gave a calibration echo at saturation level with gain reduced to give one-quarter inch of grass. Curves relating the calibration pulses to the A-scope Lucite grids are shown in Fig.(3) and Fig.(4). Magnetron frequency was checked periodically but the drift was negligible after the operating temperature had been reached.

At the observation points, the rate-recording gauges were read every minute and the drop size distribution sheets were exposed every two to five minutes depending on the rate of fall. Time records were made in seconds, so that the photographic and the meteorological data corresponded within a maximum of plus or minus fifteen seconds.

Data was taken from the A-scan pictures by projecting the 35-millimeter negative on a 24 by 36 inch screen. At fixed ranges the echo height was scaled and converted to dbm. from the calibration curves.

Drop size, in millimeters, was taken directly from the filter paper by means of a calibrated scale and the total number of drops in each group size recorded. Drop size intervals were chosen, 0.00 to 0.19, 0.20 to 0.39, etc., and the mean diameters .1, .3, .5, etc., were used in the calculation of $\sum D^6$. The rate of fall in millimeters per hour was taken directly from the rain gauge readings at the time of the filter paper exposure. The vertical speed of drops of the mean diameters was taken from the work of E. Dillon Smith, Fig.1. $\sum D^6$ was calculated for each drop-size sheet and the results are shown in Fig.6. The broken line curves are for comparison purposes only.

Calculated Echo Intensities — S-band Radar

From Equation (15),

$$P_r = 14.58 \times 10^{-7} \cdot \frac{A_e h P_o}{\lambda^4} \cdot \frac{f_o(g, h) \sum D^6}{r^2}$$

For any given radar $\frac{A_e h P_o}{\lambda^4}$ is a constant (K_s).

For $\lambda = 10$ cm., $f_o(g, h)$ may be assumed constant and equal to 0.93,

$$\text{then } P_r = K_s \frac{\sum D^6}{r^2}$$

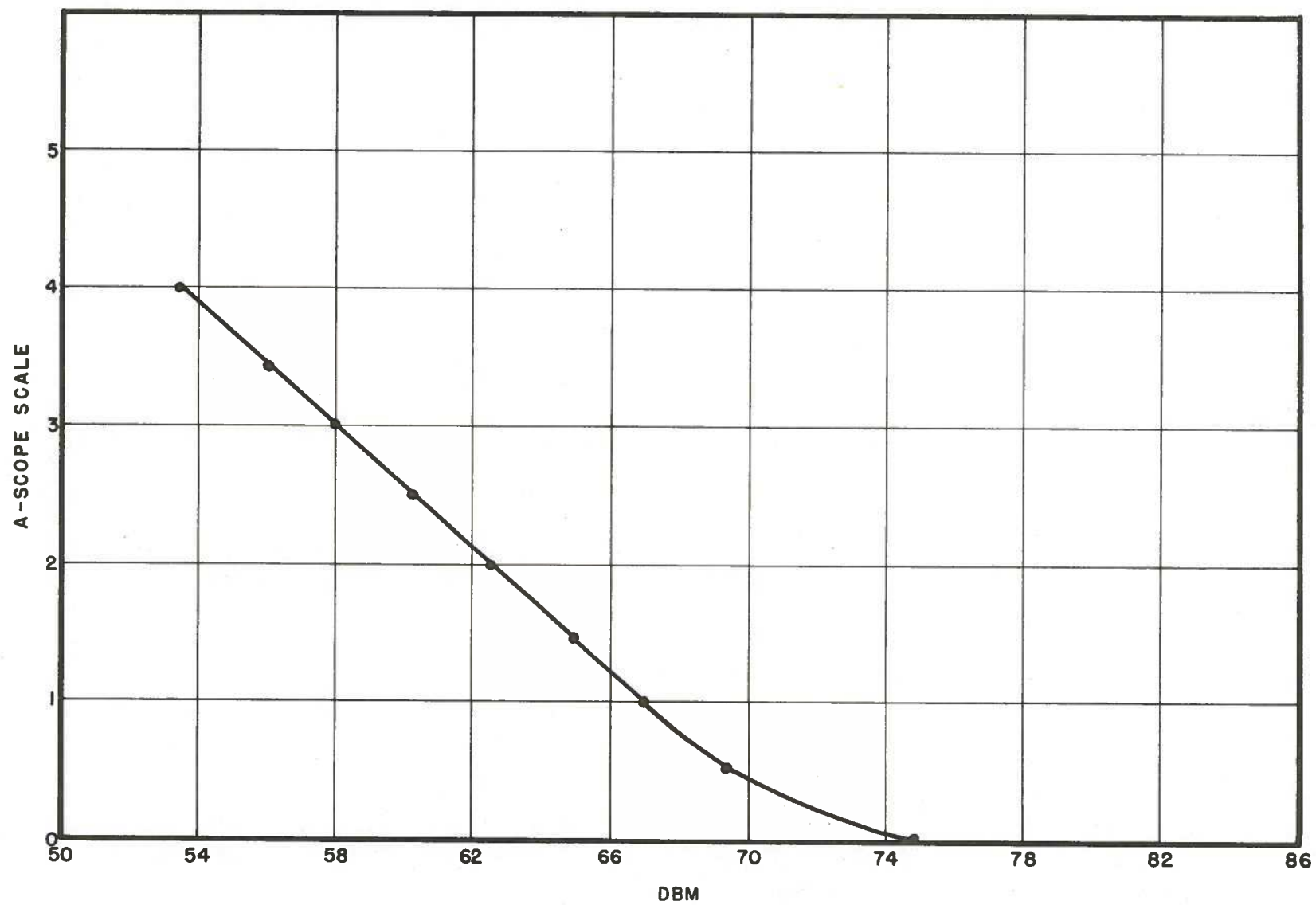


FIG. 3

S-BAND RADAR
A-SCOPE CALIBRATION

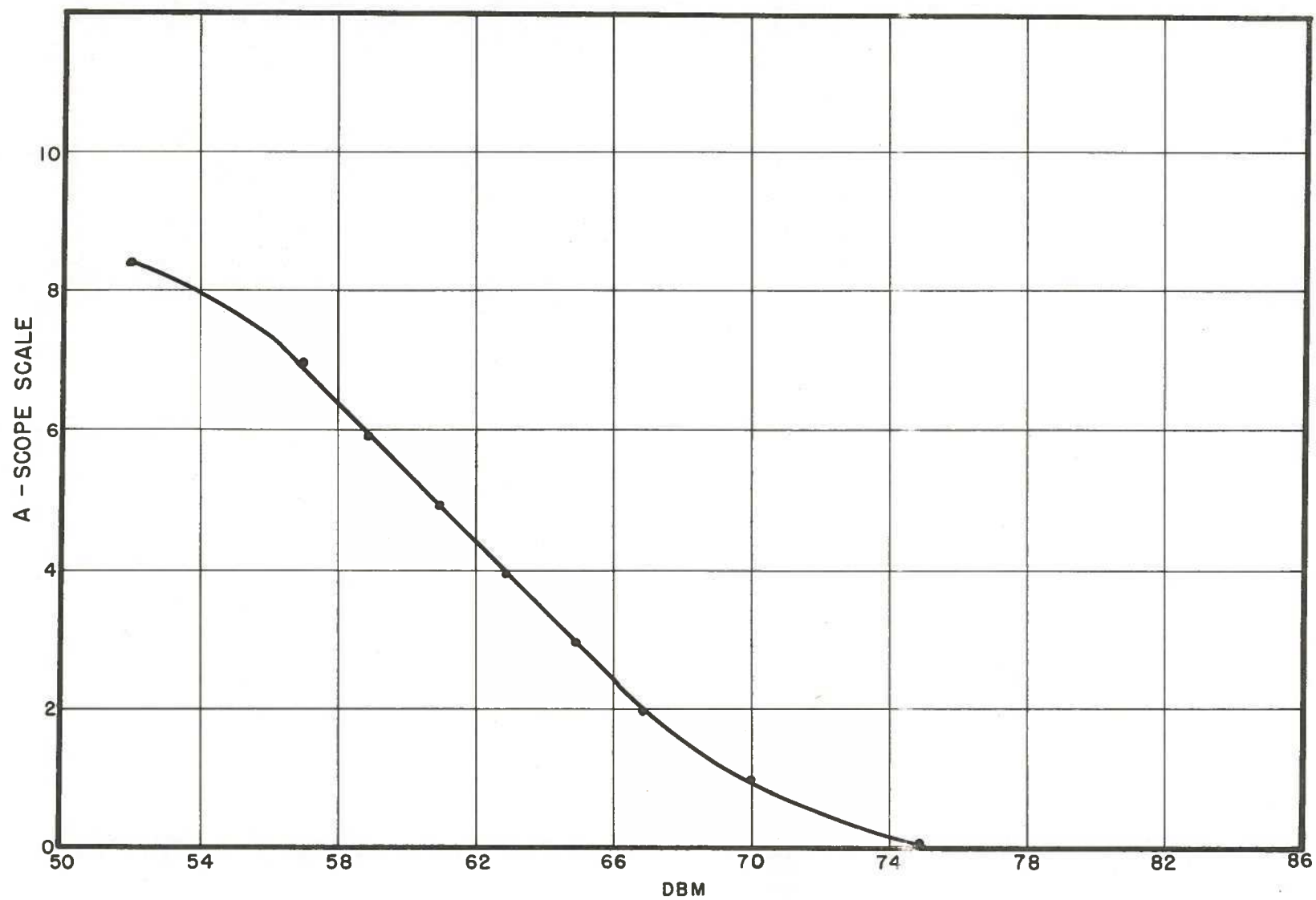


FIG.4

X-BAND RADAR
A-SCOPE CALIBRATION

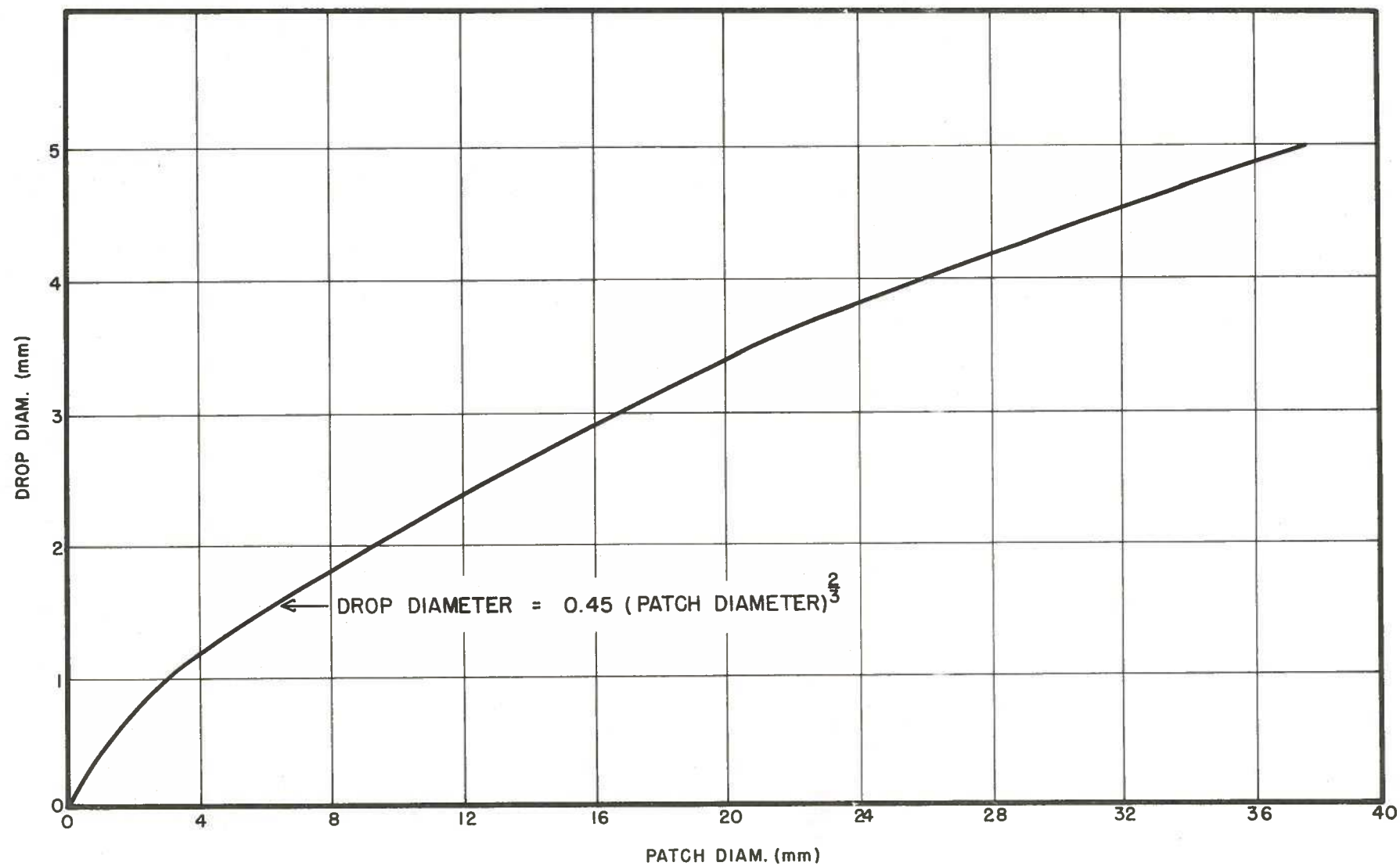


FIG. 5

CALIBRATION CURVE FOR DROP SIZE MEASUREMENTS
USING WHATMAN NO. 1 FILTER PAPER
FROM DATA BY C.A.O.R.G. (REF. (1))

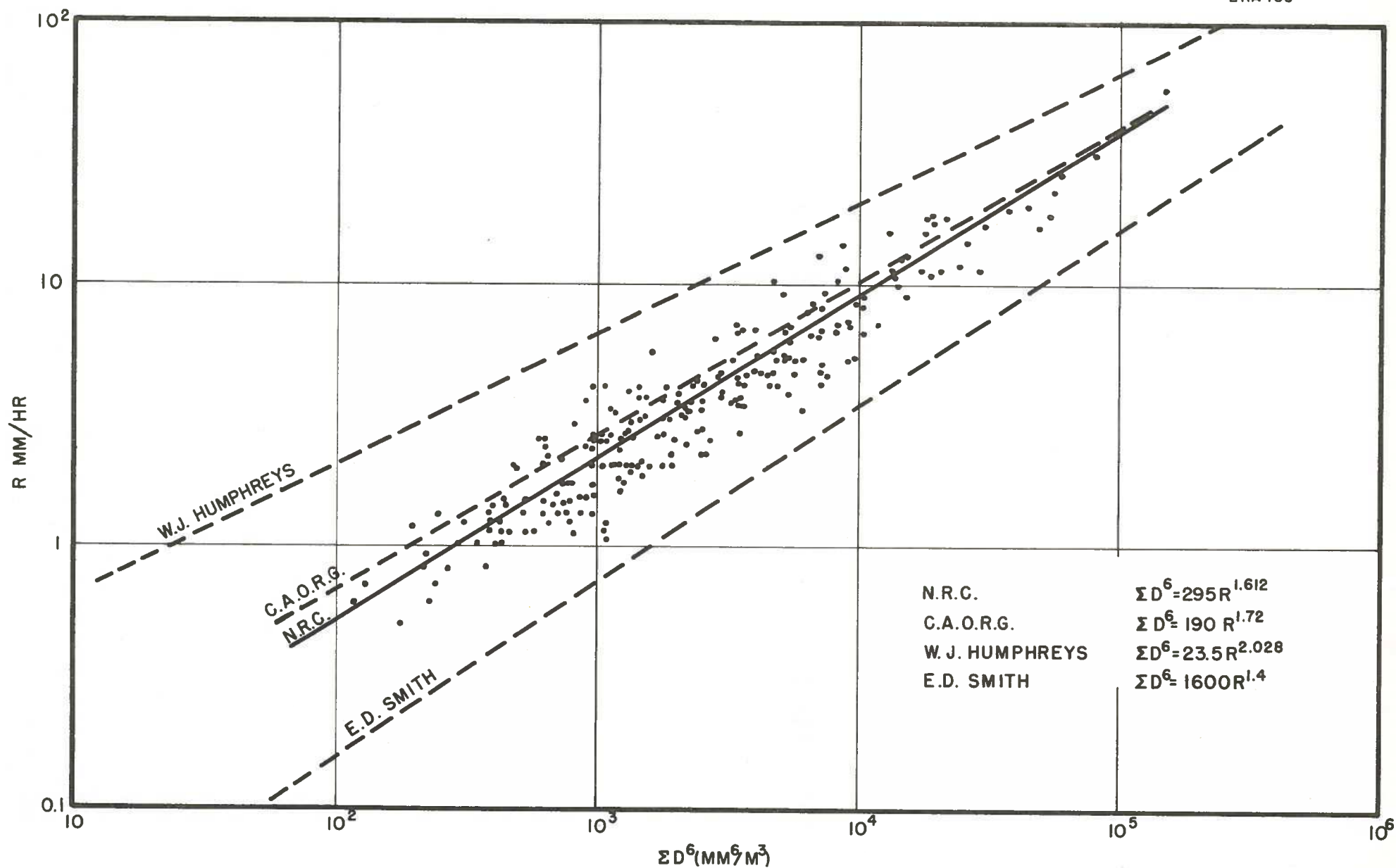


FIG. 6

For a given rate of fall ΣD^6 may be obtained from the relationship $\Sigma D^6 = 295 R^{1.612}$ (Fig.6), and received power is a function of range only.

Substituting values for the 10-centimeter radar used in the experiment,

$$\lambda = 10.0 \text{ cm. wavelength}$$

$$A_e = 1.58 \text{ m}^2 \text{ effective receiving area of antenna}$$

$$h = 0.3 \text{ km. pulse length}$$

$$P_o = 30 \text{ kw. peak power output,}$$

the expression for P_r becomes

$$P_r = 1.928 \cdot \frac{\Sigma D^6}{r^2}.$$

For example, if $R = 10 \text{ mm./hr.}$, $\Sigma D^6 = 12,000$; and if the range is taken as 10,000 yards,

$$\begin{aligned} P_r &= 2.31 \times 10^{-4} \text{ microwatts} \\ &= 66.36 \text{ dbm.} \end{aligned}$$

Echo intensity versus range for various values of R is shown in Fig. 7. Attenuation at 10 centimeters is almost negligible and the locus for each value of R is a straight line.

Calculated Echo Intensities — X-band Radar

Similar calculations were made for the X-band radar with the values used in the experiment and the results are shown in Fig.8. Values of $f_o(g,h)$ were obtained from Equation (4) and were found to decrease from 0.93 for $R = 1 \text{ mm.}$, to 0.777 for $R = 5 \text{ mm.}$ \square was calculated from Humphreys' typical drop size values. Attenuation was taken into account in plotting the curves, assuming a constant rate of fall over the radar path. In plotting the locus for each value of R , the deviation from a straight line is due entirely to attenuation.

From Equation (15),

$$\begin{aligned} P_r &= 14.58 \times 10^{-7} \cdot \frac{A_e h P_o}{\lambda^4} \cdot \frac{f_o(g,h) \Sigma D^6}{r^2} \\ &= K_x \cdot \frac{f_o(g,h) \Sigma D^6}{r^2} \end{aligned}$$

ERA 180

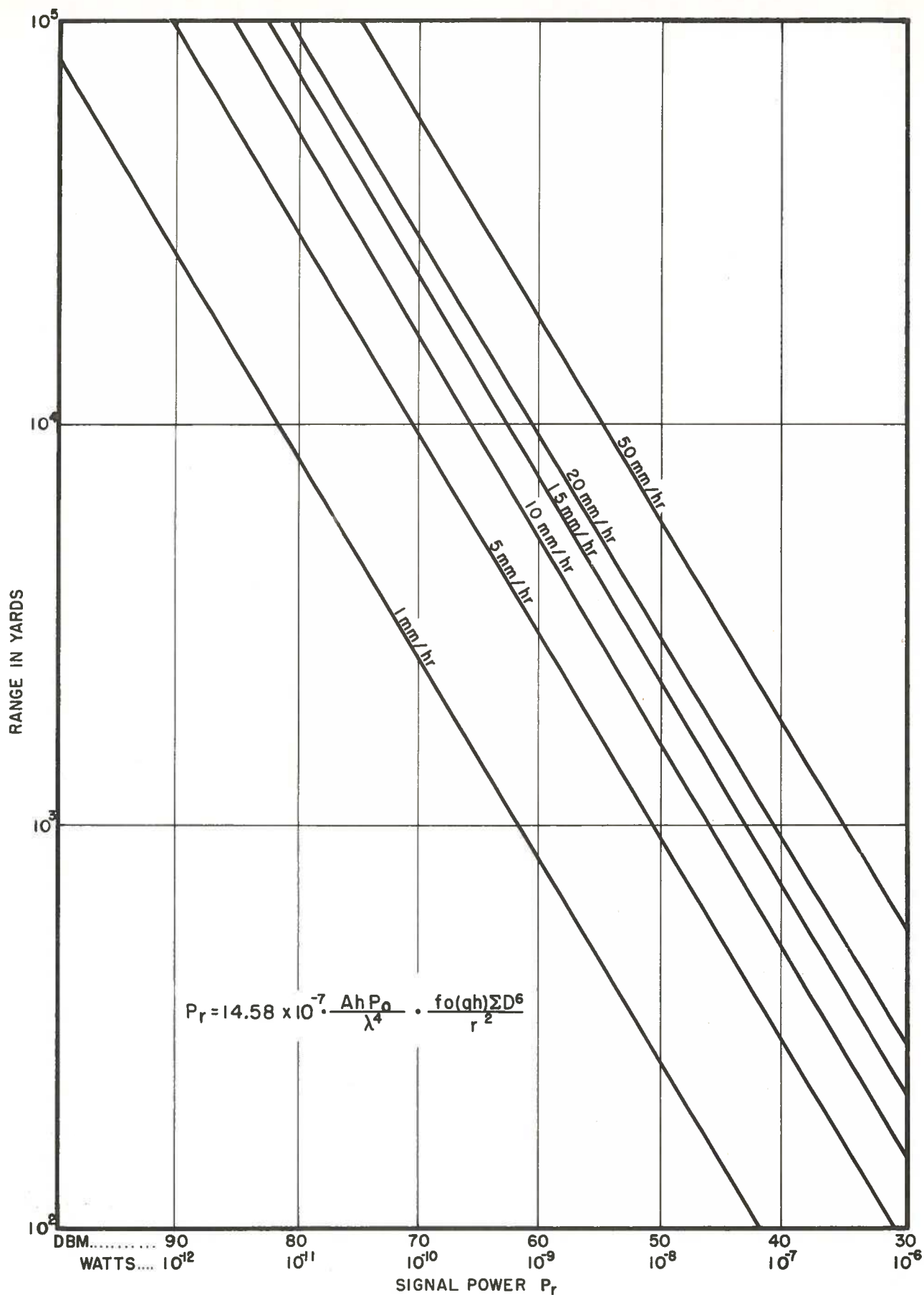


FIG. 7
S - BAND
RAIN ECHO INTENSITY VERSUS RANGE
FOR VARIOUS PRECIPITATION RATES

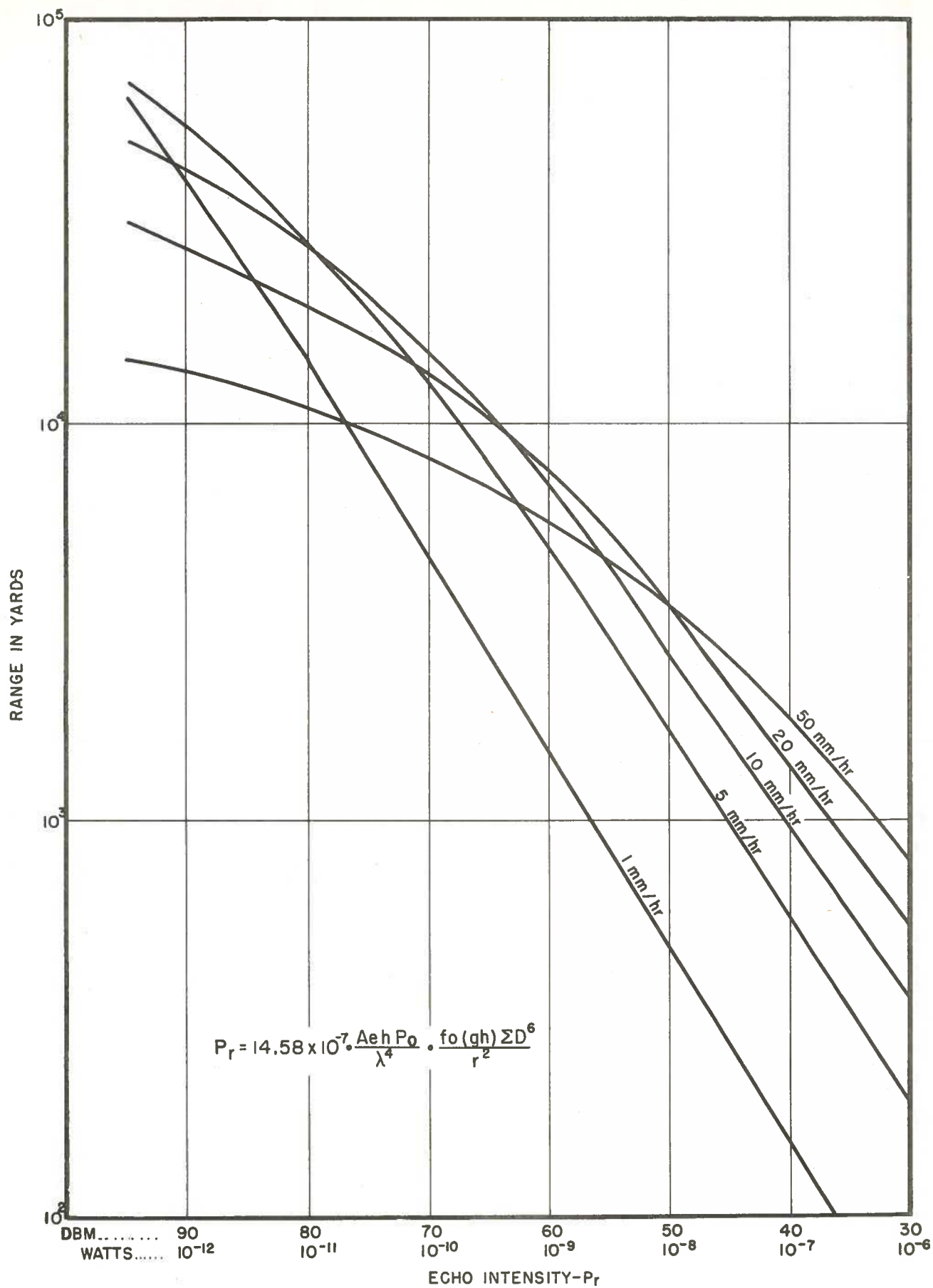


FIG. 8

X-BAND RADAR

RAIN ECHO INTENSITY VERSUS RANGE

Substituting values for the 3-centimeter radar used in the experiment,

$$\begin{aligned}\lambda &= 3.00 && \text{wavelength} \\ A_e &= 0.273 \text{ m}^2. && \text{effective receiving area of antenna} \\ h &= 0.225 \text{ km.} && \text{pulse length} \\ P_o &= 7.5 \text{ kw.} && \text{peak power output,}\end{aligned}$$

it is found that

$$\begin{aligned}K_x &= 8.28, \\ \text{so that } P_r &= 8.28 \frac{f_o(g,h) \Sigma D^6}{r^2}.\end{aligned}$$

For $R = 10 \text{ mm./hr.}$, and a typical drop diameter $D = 1.3 \text{ mm.}$,

$$\alpha = \frac{\pi D}{\lambda} = 0.136,$$

and from Equations (4) and (7),

$$f_o(g,h) = 0.88.$$

Also, from Fig.6, $\Sigma D^6 = 12,000$.

Then for a range of 10,000 yards, and a rainfall of 10 mm./hr.,

$$\begin{aligned}P_r &= 8.28 \times \frac{.88 \times 12,000}{10^8} = 8.75 \times 10^{-4} \text{ \mu watts} \\ &= 60.58 \text{ dbm.}\end{aligned}$$

From Ryde's values for attenuation (see Ref.4) for a rainfall of 10 mm./hr., the attenuation is 0.38 db. per 1000 yards (radar path).

Therefore, at the range 10,000 yards,

$$P_r = 60.58 \text{ dbm.} + 3.8 \text{ dbm.} = 64.38 \text{ dbm.}$$

Experimental Results

The values of ΣD^6 (Fig. 6) were calculated from various types of rainfall varying in rate from 1 to 3 mm./hr. for a light rain, to 50 mm./hr. in heavy thunder showers. 270 samples, taken from 7 different rainstorms, all fall in a reasonably narrow band about the locus $\Sigma D^6 = 295 R^{1.612}$. This agrees very closely with the results obtained by CAORG (1) using the same technique. The locus $\Sigma D^6 = 190 R^{1.72}$ is shown in Fig. 6 for comparison purposes. The results of the two separate experiments indicate that, with sufficient experimental work, a fixed relationship between ΣD^6 and R could be established that would be accurate for all radar measurements.

The loci (Fig. 6) of Humphreys and Smith were calculated from their respective precipitation tables, listing median drop size for given rates of fall. Both curves fall outside the band of experimental points and it is apparent that the concept important to radar, ΣD^6 , can not be determined from precipitation tables.

Quantitative measurements of P_r (echo intensity), for S-band radar, versus ΣD^6 are shown in Fig. 9. The locus shown is not necessarily the best but has been drawn to parallel the theoretical locus obtained from data shown in Fig. 7. These results are low by 4.5 decibels on the average. This error was consistent throughout all experiments and can only be accounted for by a fixed error in radar calibration or in the method of measuring ΣD^6 .

Fig. 10 is a duplicate of the same data taken on X-band radar. The theoretical curve assumes continuous rainfall over the radar path. This was never found to be the case except at very low rates of fall of the order of 1 or 2 mm./hr. As shown in Fig. 10 for $\Sigma D^6 = 20,000$, corresponding to $R = 15$ mm./hr., errors of 10 db. were recorded. The locus of the curve tends to ignore these points and the position is dictated by the more accurate results obtained at the lower rates of fall.

Identical X-band and S-band A-scan photographs taken during the storm of October 8 are shown in Figs. 11 and 12 with their associated data.

Figs. 13 and 14 are examples of excessive rainfall. The rate at the radar site was 52 mm./hr., decreasing along the path to 39 mm./hr. at the half-way point, and down to 31 mm./hr. at the Rouge Hill site. In the X-band picture the Bluff echoes at 8,000 yards have almost disappeared and the target echo at 13,500 yards is completely masked. On S-band, the rain echoes are at saturation level to 4,000 yards and are still visible at 16,000 yards with no sign of attenuation in echoes at 26,000 yards. Fig. 15 shows the results obtained from the S-band data. The average measurement was within 3 decibels of the calculated values.

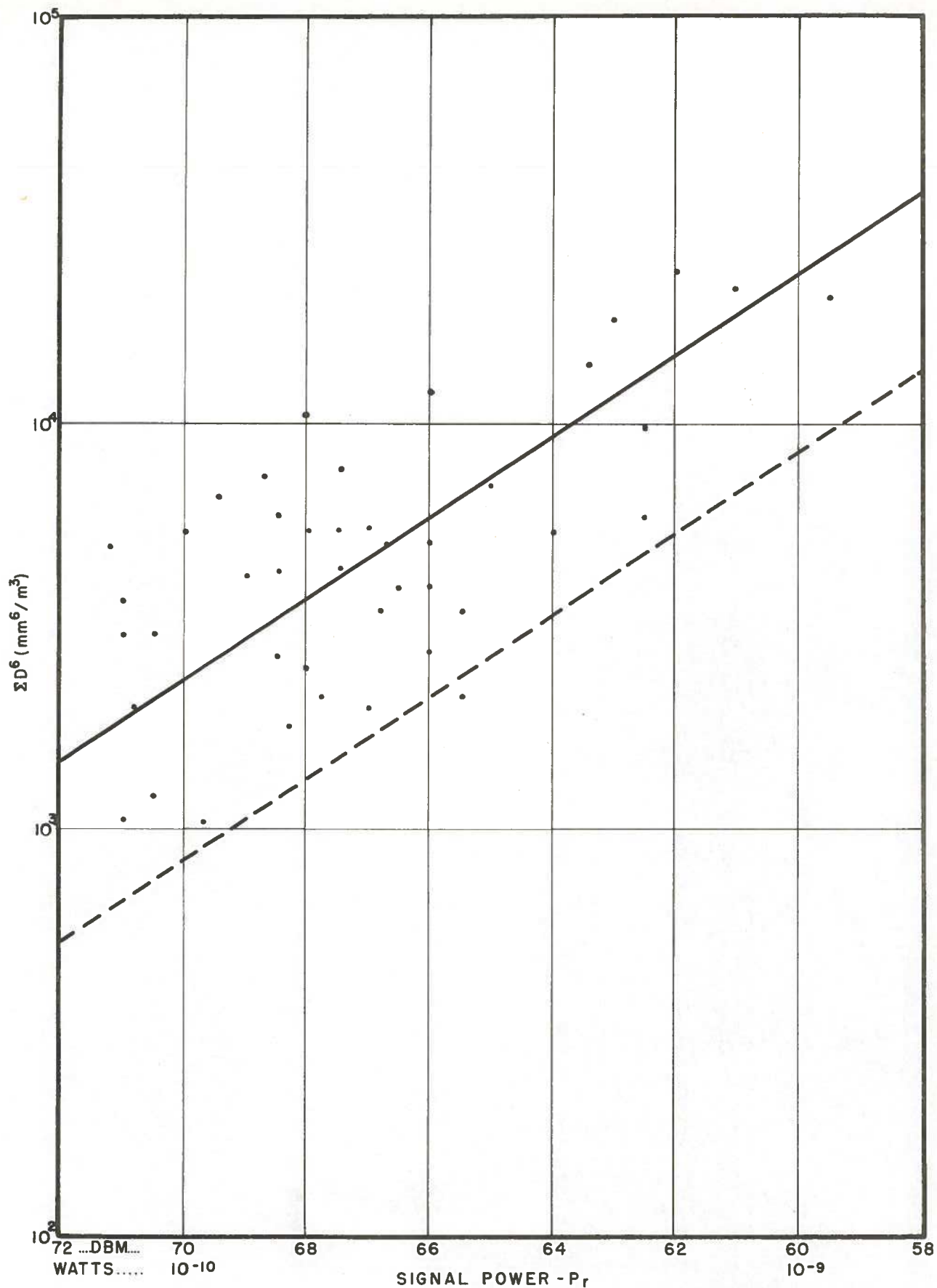


FIG. 9
S-BAND
RAIN ECHO INTENSITY VERSUS ΣD^6
AT 4000 YARDS RANGE
 $P_0 = 30$ KW (TRANSMITTED POWER)

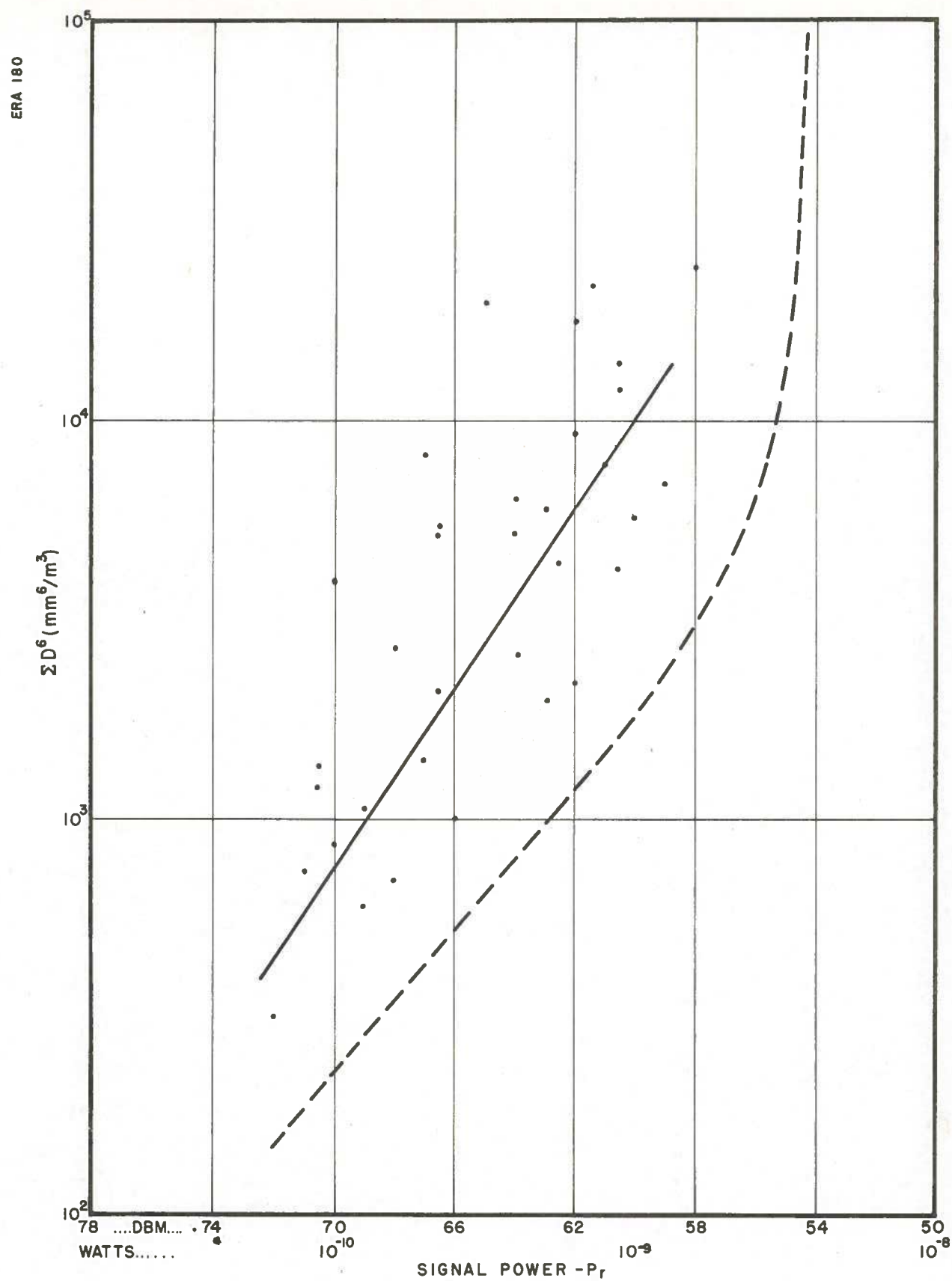
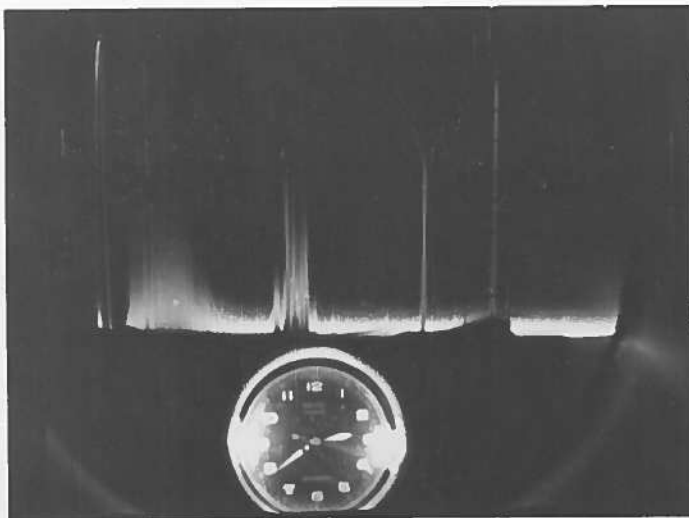


FIG. 10

X - BAND

RAIN ECHO INTENSITY VERSUS ΣD^6
AT 4000 YARDS RANGE

$P_0 = 7.5 \text{ KW}$ (TRANSMITTED POWER)



X-band
 P_r - 62 dbm.

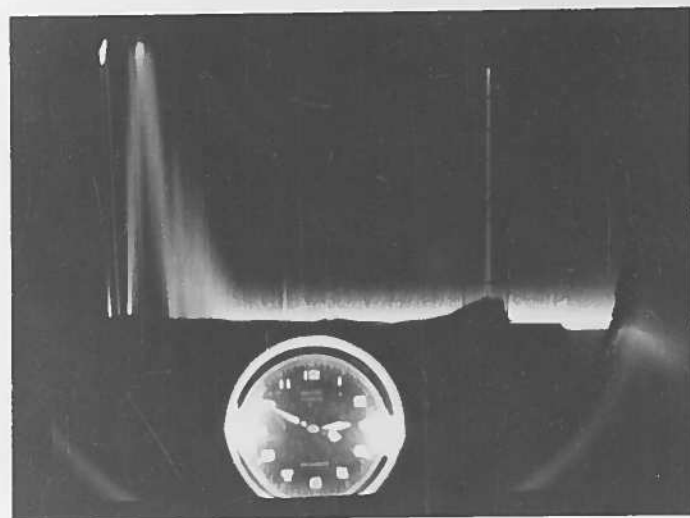
Fig. 11

Date -Oct. 8, 1948
 Time -1439 hrs.
 Range -4,000 yds.
 R -7.6 mm./hr.
 ΣD^6 -7,600



S-band
 P_r - 64 dbm.

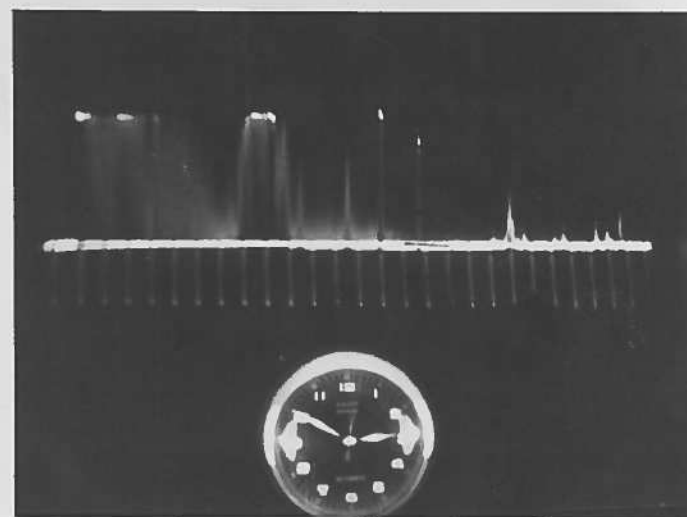
Fig. 12



X-band
 P_r - masked

Fig. 13

Date -Nov. 20, 1948
 Time -0250 hrs.
 Range -13,500 yds.
 R -31 mm./hr.
 ΣD^6 -72,000



S-band
 P_r - 66 dbm.

Fig. 14

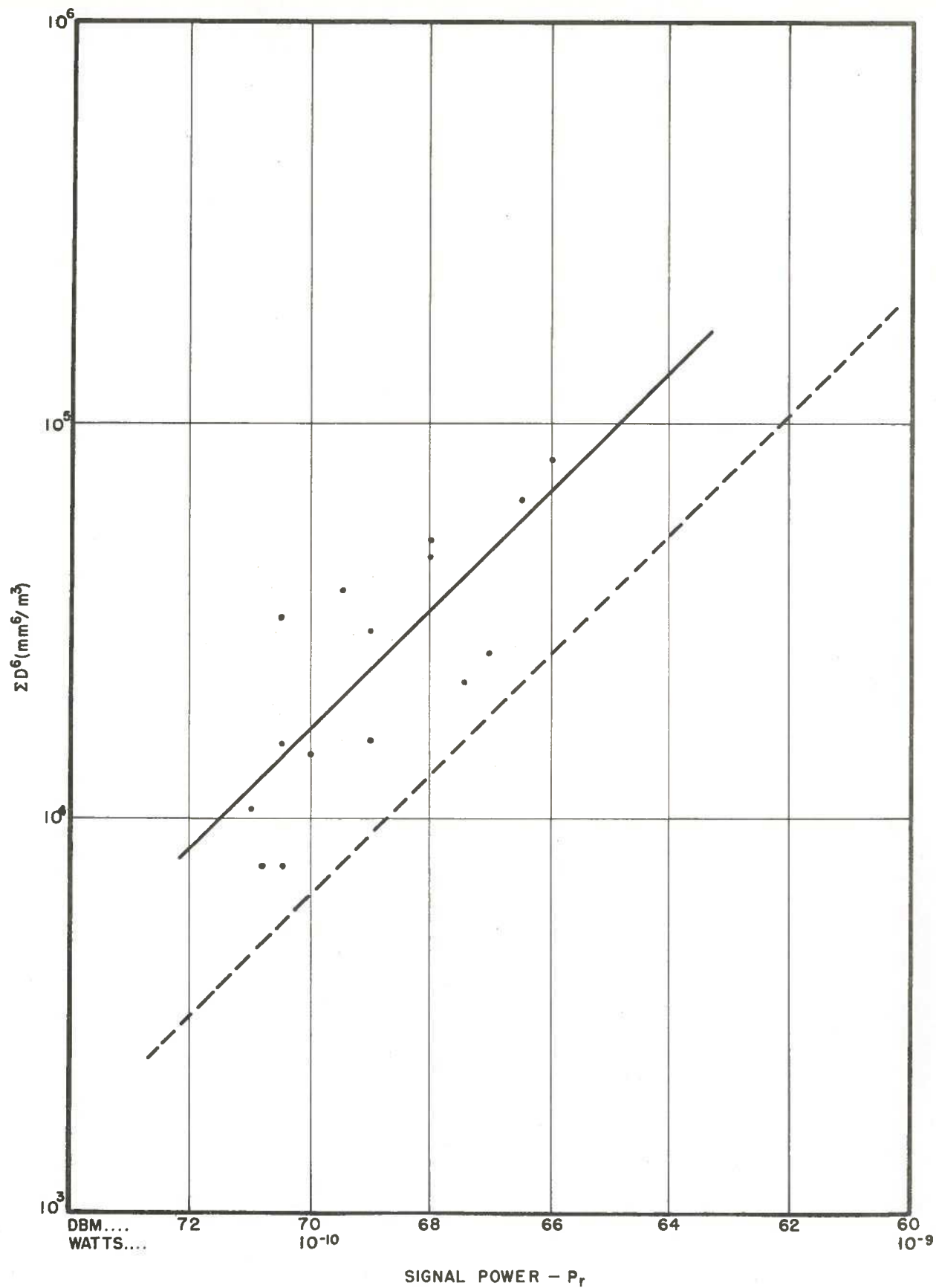


FIG. 15

S - BAND

RAIN ECHO INTENSITY VERSUS ΣD^6
 AT 13500 YARDS RANGE
 $P_0 = 30$ KW (TRANSMITTED POWER)

V

CONCLUSIONS

From the results obtained in the above quantitative measurements, the following conclusions seem reasonable:

The value of R can be measured by S-band radar within an accuracy of 25 per cent, with range limitations controlled by the radar equipment.

Except at ranges under 10,000 yards and rates of fall less than 5 mm./hr., X-band radar cannot be used for rainfall measurements with any degree of accuracy.

From comparison of X-band and S-band clutter signals, it appears that an intermediate frequency could be used to advantage in meteorological work. This would necessarily have to be a compromise between the size of the antennas, bulk and power requirements of S-band radar, and the excessive attenuation caused by precipitation on X-band.

Following the same theory as that used to calculate rain echo intensity at a given range, it is possible to forecast the detection ranges of typical targets under known weather conditions. Such forecasts would be advantageous for marine navigation in fog or rain, especially where buoys or other markers are equipped with reflectors.

VI

ACKNOWLEDGMENT

The assistance of the Meteorological Division of the Department of Transport and the Canadian Army Operational Research Group is gratefully acknowledged.

REFERENCES

1. Canadian Army Operational Research Group, Measurement of Rainfall by Radar, Report no.47, Sept.,1947.
2. J.W. Ryde, Echo Intensities and Attenuation due to Cloud, Rain, Hail, and Dust Storms at Centimeter Wavelengths, Research Laboratories of the General Electric Company, Report no.7831.
3. J.W. Ryde, Attenuation of Centimeter Waves by Rain, Hail and Clouds, Research Laboratories of the General Electric Company, Report no.8516.
4. J.W. Ryde, Attenuation of Centimeter and Millimeter Waves by Rain, Hail, Fogs and Clouds, Research Laboratories of the General Electric Company, Report no.8670.
5. E. Dillon Smith, Notes on Rain Drop Sizes and Attenuation of one-way Microwave Radio Transmission, Third Conference on Propagation, Nov.,1944, Washington, D.C.
6. J.E.N. Hooper and A.A. Kippax, Interim Report on Measurements of Radar Intensities from Rain and Snow, T.R.E. Report T2082, July, 1947.
7. J.E.N. Hooper and R.A. Smith, Measurement of Radar Echo Intensities from Precipitation, T.R.E. Report T2116, Nov.,1946.
8. A.C. Best, Size Distribution of Raindrops, Part 2, Meteorological Research Committee, MRP452, Dec.,1948.
9. Meteorological Factors in Radio Wave Propagation, published by the Physical Society, London, April,1946.

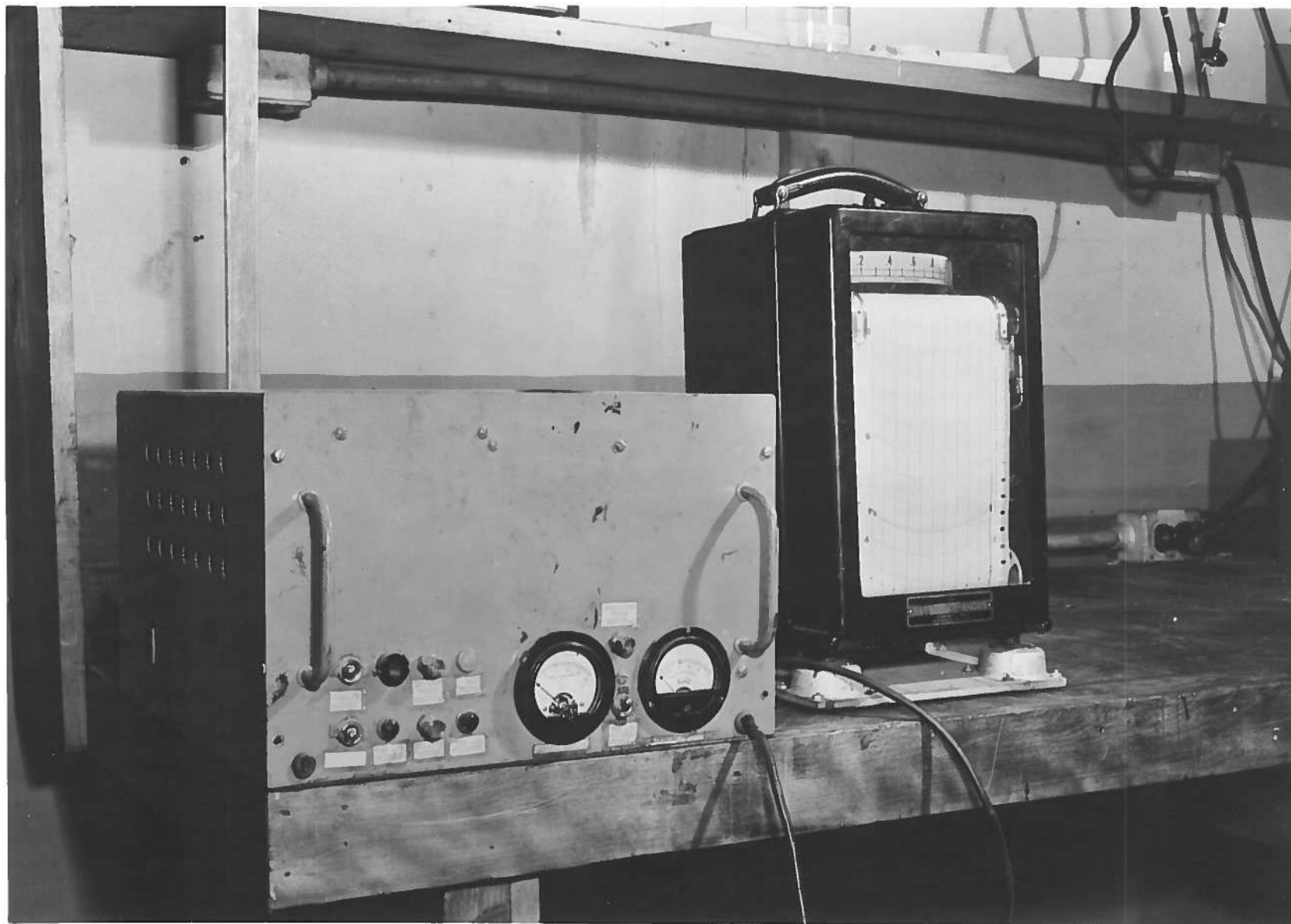


Photo 1
X/S Trails - X-band Field Strength Recorder
Rouge Hill Site

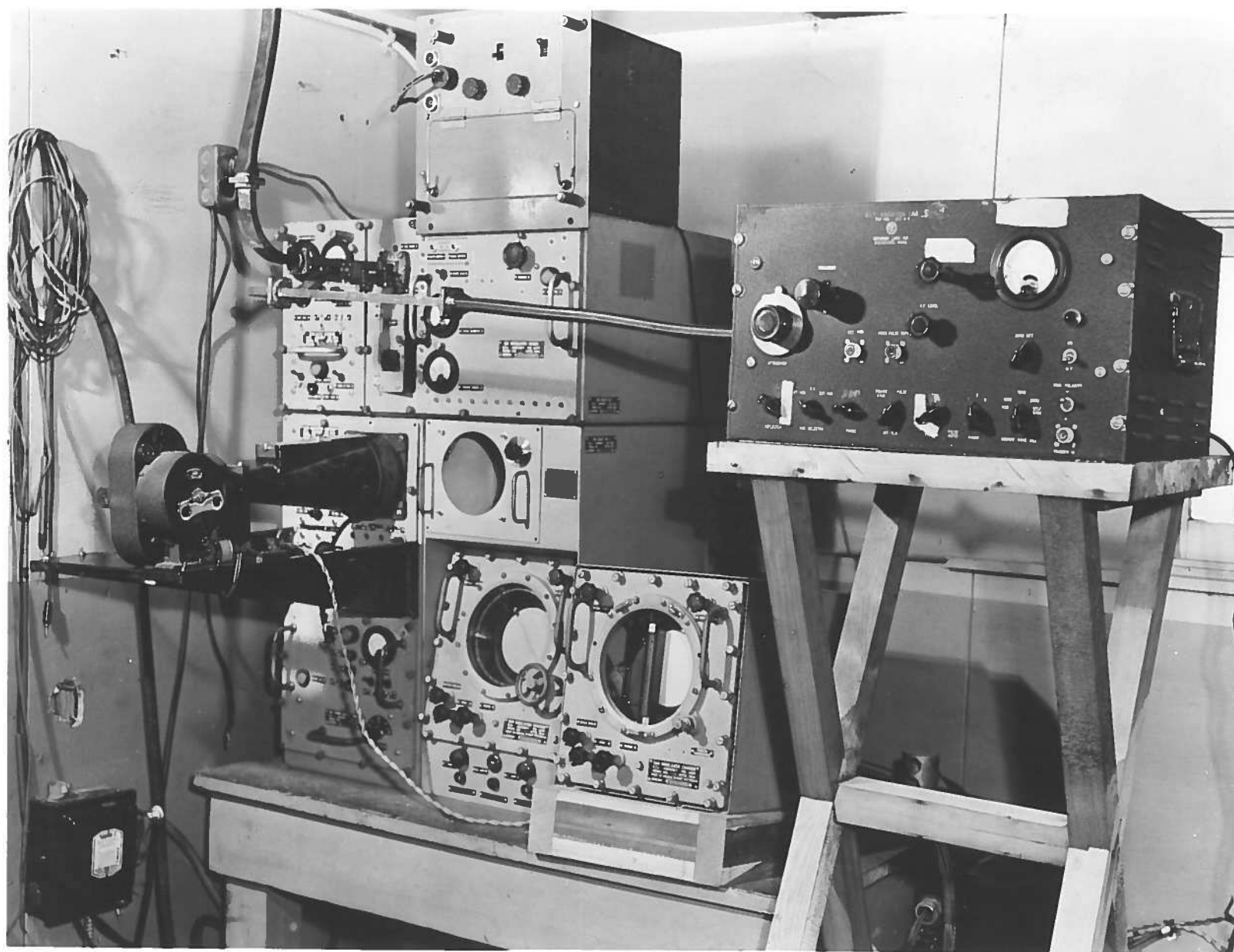


Photo 2
X-band Radar with Calibrating and Photographing Equipment
Scarboro Site

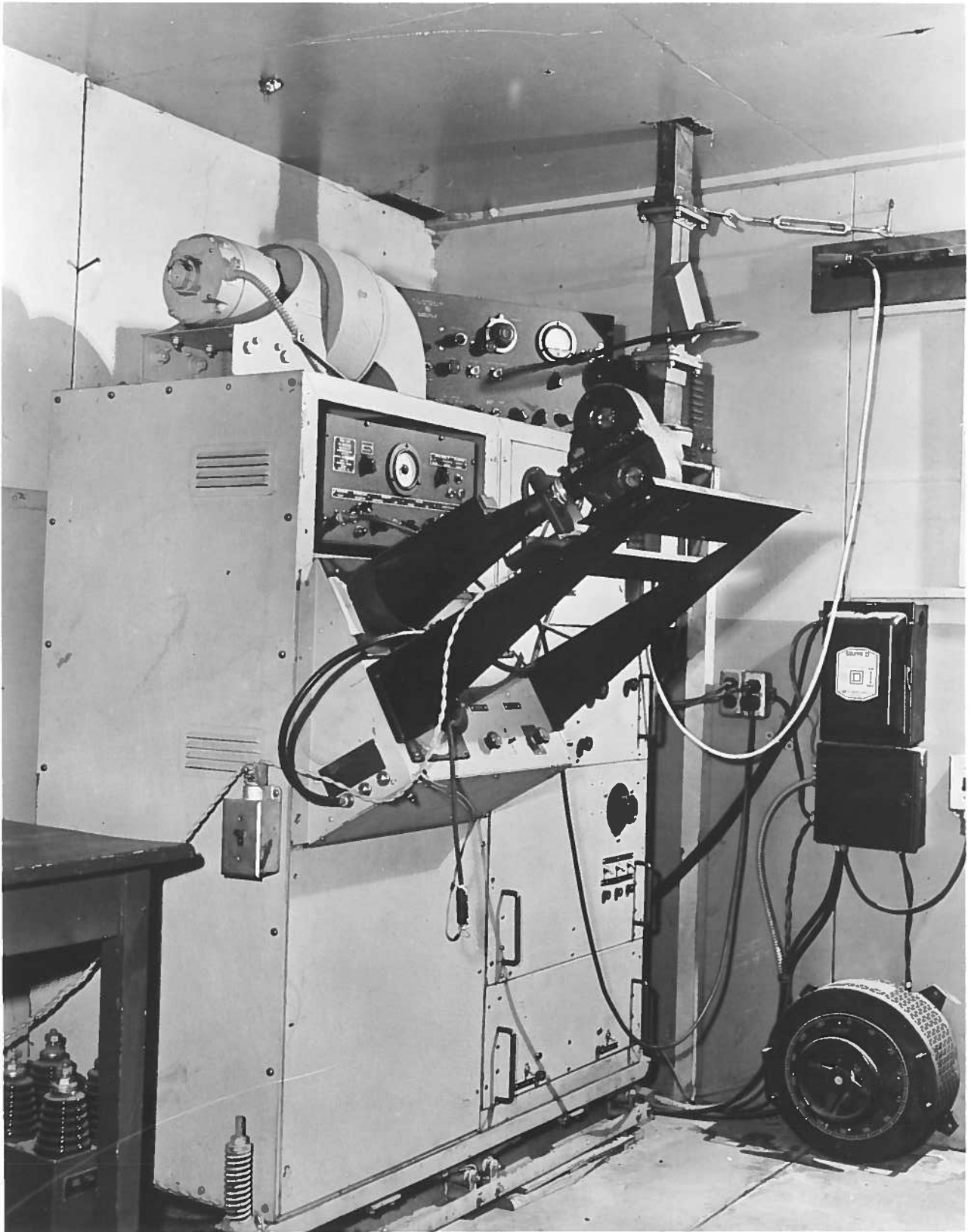


Photo 3
S-band Radar with Calibrating and Photographing Equipment
Scarboro Site



Photo 4
S-band and X-band Radar Antennas

NFB Photo



Photo 5
Rain Gauge and Nifer Screen

NFB Photo

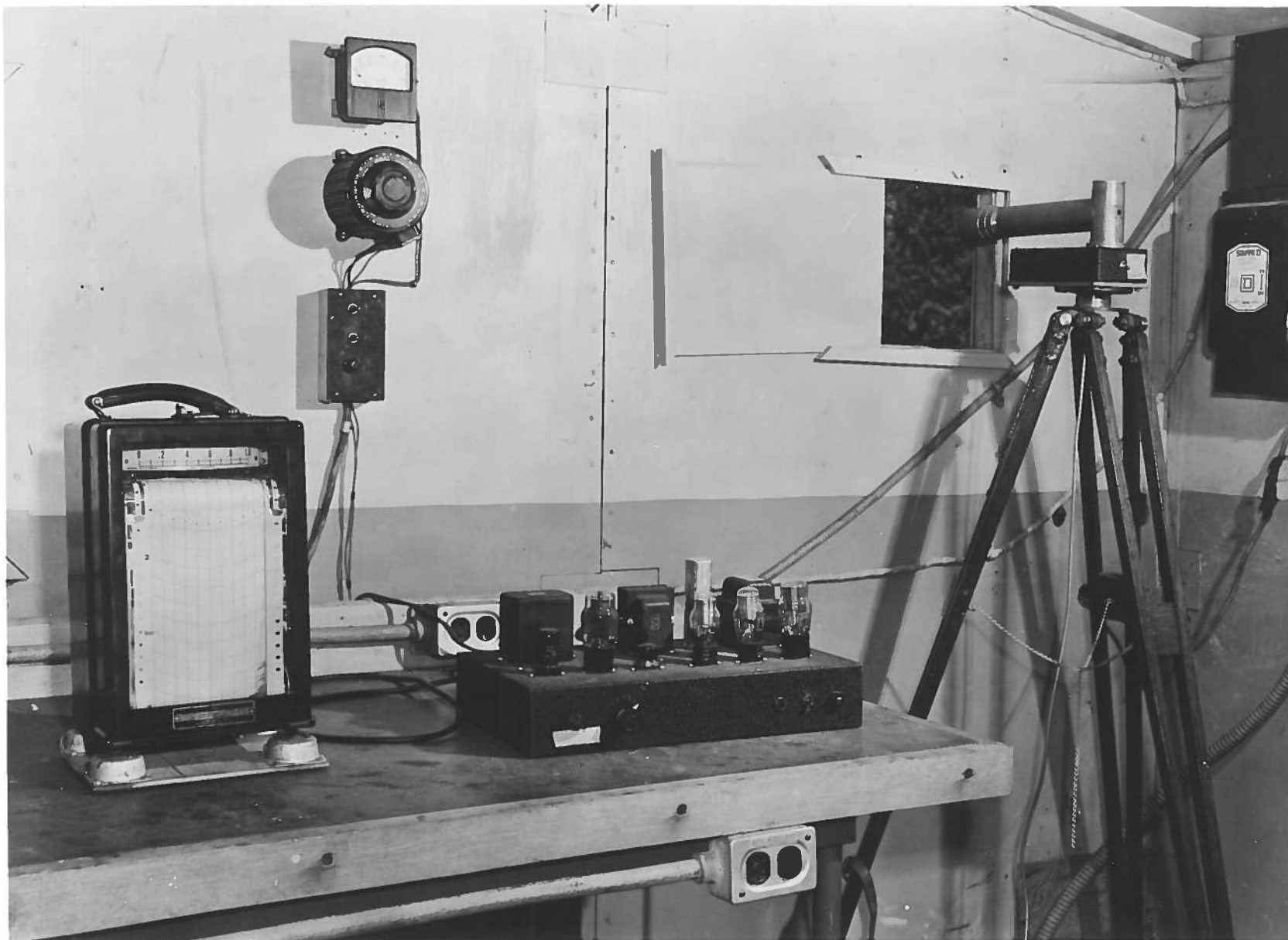


Photo 6
Photoelectric Recording Densitometer

NFB Photo



Photo 7
Eight-foot Corner Reflector and Observation Station
Rouge Hill Site